Geofísica Internacional (1996), Vol. 35, Num. 2, pp. 175-188

Subsurface flow generation in an experimental plot during applied rainfalls in the Ouachita mountains of Arkansas

José Návar[1], Edwin L. Miller[2] and Donald J. Turton[2]
[1] *Facultad de Ciencias Forestales, Universidad Autónoma de Nuevo León, Linares, N.L.*
[2] *Dept of Forestry, Oklahoma State Univ., Stillwater.*

Received: October 25, 1994; accepted: January 12, 1996.

RESUMEN

Este reporte enfatiza la importancia relativa de la intensidad de la lluvia y de los potenciales del agua del suelo previos a la aplicación de la lluvia en procesos del flujo de agua a través de los macroporos del suelo a escalas espaciales relativamente cortas en cuencas forestales de las Montañas Ouachita de Arkansas. Los potenciales del agua, los contenidos del agua del suelo, el flujo subsuperficial y las concentraciones de bromo fueron medidas en un sitio forestal experimental en las Montañas Ouachita de Arkansas durante la aplicación de 17 tormentas. Las tormentas tuvieron duraciones desde 0.8 hasta 4.25 h e intensidades desde 10 hasta 75 mm h^{-1} y fueron aplicadas con bromo durante el período de julio 17 a octubre 10 de 1991. Los potenciales del agua previos a la aplicación de la lluvia tuvieron un rango desde -90 hasta -10 cm de agua y desde -29 hasta +19 cm de agua arriba de los 50 y 80 cm de profundidad del suelo, respectivamente. Los contenidos del agua del suelo variaron desde 0.23 hasta 0.36 cm cm^{-3} arriba de los 50 y 80 cm de profundidad del suelo, respectivamente. Los resultados mostraron que el flujo subsuperficial total varió desde 82 hasta 24% del total de la lluvia aplicada. Aunque el suelo a 80 cm estuvo saturado para 11 tormentas, la mayoría del flujo subsuperficial se presentó en el horizonte superior del suelo para la mayoría de las lluvias. Los parámetros de los hidrogramas de corrientes obtenidos se relacionaron estadísticamente con la tasa de aplicación de la lluvia y con el potencial del agua del suelo. Los concentraciones de bromo indicaron que el escurrimiento subsuperficial estuvo compuesto principalmente por el agua aplicada o agua nueva, indicando que esto ocurre preferencialmente y que es un proceso común en el sitio experimental.

PALABRAS CLAVE: Flujo subsuperficial, flujo a través de los macroporos, intensidad de la lluvia, potencial del agua del suelo.

ABSTRACT

This paper addresses the relative importance of rainfall intensity and pre-storm soil water potentials in macropore flow processes at short spatial scales in forested watersheds in the Ouachita Mountains of Arkansas. Soil water potentials, soil moisture contents, lateral subsurface flow, and runoff bromide concentrations were monitored in an experimental forest soil block in the Ouachita Mountains of Arkansas for 17 applied rain storms. Rainfalls were of durations of 0.82 to 4.25 hours in length with intensities from 75 to 10 mm h^{-1} and were applied with bromide concentrations during July 17 to October 10 of 1991. Pre-storm soil water potentials ranged from -90 to -10 and from -29 to +19 cm of water above 50 and 85 cm of soil depth, respectively. Pre-storm soil moisture contents ranged from 0.23 to 0.36 cm^3 cm^{-3} above 50 and 85 cm of soil depth, respectively. The results showed that total subsurface flow averaged from 82% to 24% of total applied rainfall. Even though soil saturation was observed at the bottom of the soil block for 11 experimental runs, most runoff occurred as shallow subsurface flow for most applied storms. Hydrograph parameters were statistically related to the rate of rainfall input and to pre-storm soil water potential. Bromide concentrations in subsurface flow indicated that most lateral subsurface flow was composed of new water, indicating that preferential flow was a common process in the experimental plot.

KEY WORDS: Subsurface flow, macropore flow, rainfall intensity, soil water potential.

INTRODUCTION

The mechanisms of stormflow generation in undisturbed forest watersheds have been a cause of major concern during the last four decades. Environmentally-related processes, such as damaging floods and the fate of chemicals within soils, have prompted renewed trends in forest hydrology. Hewlett and Hibbert (1963); Whipkey (1965); Dunne and Black (1970a and 1970b); Beasley (1976); and Anderson and Burt (1978) observed runoff processes in experimental forest plots. Subsurface flow, return flow, and saturated flow are currently considered physical streamflow generating processes in the hydrologic literature (Dunne and Leopold, 1978). The dominance of these new mechanisms of runoff production has been identified in terms of soils, vegetation and climate.

Upland forest watersheds of the Ouachita Mountains generate stormflow following the variable area source concept through subsurface flow (Williams, 1990 and Turton *et al.* 1992). Because subsurface flow contributes up to 70% to stormflow (Turton *et al.*, 1992) and runoff responds rapidly to rainfall input (Beasley, 1976 and Turton *et al.*, (1992), this type of flow requires an efficient drainage mechanism (Beasley, 1976; Miller *et al.* 1988 and Turton *et al.* 1992).

Recent research on subsurface flow has indicated that macropores play an important role in subsurface flow processes (Mosley, 1979; 1982; Beven and Germann, 1982; Germann, 1990; McDonnell, 1990 and McDonnell *et al.*, 1991). Macropores are soil structures that permit a type of non-equilibrium channeling flow (Beven and Germann,

1982) and provide preferential flow paths so that mixing and transfer between macropores and matrix pores is limited (Skopp, 1981).

Chemical observations of subsurface flow have theoretically refuted the interpretation that macropores contribute to rapid stormflow generation. Conflicting natural stable isotopes and chemical tracing studies conducted by Sklash *et al.*, (1986) at the Maimai catchment in New Zealand observed that old, stored, water dominated throughflow in all storm events monitored. However, McDonnell (1990) reconciled water chemistry and macropore flow studies by proposing a mechanism for macropore flow of old water, where bypass flow, slope water table development, and lateral pipe flow enabled large volumes of stored water to be delivered to a first-order channel bank.

According to the model proposed by McDonnell (1990), macropore flow at both short and large spatial scales is driven by rainfall intensity and pre-storm soil water potential. The objective of this study was to examine how rainfall intensity and pre-storm soil water potentials control preferential flow at short spatial scales in an experimental forest plot in the Ouachita Mountains of Arkansas.

MATERIALS AND METHODS

The study area

An experimental plot was established 35 miles north of Hot Springs, Arkansas, in the U.S Forest Service Alum Creek Experimental Forest in the Ouachita Mountains of Arkansas. The soils on the Alum Creek experimental watersheds are classified by the USDA Forest Service as the Alemance associations (Typic Hapludults). DeWitt and Steinbrenner (1981) classified the soil as the Sandlick Series. The general soil slope for the experimental plot was 16%. The soil description of the area, textural and bulk density analyses are reported in Table I.

The vegetation of the Alum Creek Watersheds is classified as an association of Loblolly-Shortleaf pine, *Pinus taeda-Pinus echinata* and hardwoods, *Quercus alba, Quercus rubra, Cornus florida, Acer rubrum, Carya spp and Nyssa silvatica.*

The climate of the area is temperate-humid with an annual average temperature of 23.5°C, ranging from 11.5°C in January to 34.0°C in August. The mean annual precipitation is 1250 mm, of which 33% occurs during April through June. There is no well defined dry season, however, summer precipitation is highly variable and high rates of summer evapotranspiration cause frequent soil moisture deficits.

The experimental plot

An experimental plot 6.3 m in length by 2.05 m in width, with a 0.5 m buffer strip zone on each side, was hydrologically isolated by digging a trench down to the C soil horizon (0.90 to 1.1 meters) (Figure 1). The side and upslope walls were sealed with polyethylene sheets, while the lower wall was left uncovered for sample collection and observations during sprinkling experiments. Perforated pipes were laid at the bottom of the upper and two side trenches and covered with 35 cm of gravel to allow drainage around the experimental plot. The remainder of the trench was filled with the original soil to provide support to the experimental block. The site was cleared of all shrubby and large trees.

The experimental plot was instrumented with three sets of tensiometers and four subsurface flow collectors. A rainfall simulator was constructed to sprinkle the plot and the buffer area. A tarp was also set up at a height of approximately 1.80 m to prevent direct throughfall from natural rainfall into the experimental plot.

Subsurface flow collectors

The system to measure subsurface flow at the lower open cross sectional area of the experimental plot, C.S.A., 13635 cm^2, was constructed as described by Turton *et al.*, (1992). It consisted of four troughs placed at 14, 26, 44 and 67 cm of soil depth. The first trough collected water from the Litter, A and E soil horizons, C.S.A.=2680 cm^2, the second and third troughs from the B1, C.S.A.=2375 cm^2, and B2, C.S.A.=3870 cm^2, soil horizons, and the last immediately above the interface between the B and C soil horizons, C.S.A.=4710 cm^2.

Troughs were constructed by cutting 0.11 X 2.1 m PVC drain pipe lengthwise. Polyethylene sheeting was inserted horizontally into the soil to a depth of approximately 5 cm to direct collected subsurface flow from the soil horizon into the troughs. Flow collected from each trough was drained into a recording individual tipping bucket. A data logger recorded the number and time of tips for each tipping bucket.

Soil water pressures

Soil water pressures were measured with pressure transducers and mercury-water manometers connected to custom-made tensiometers. Tensiometers were constructed, following the design of Cassel and Klute (1986). Eighteen of these devices were installed on the experimental plot in the fall of 1990: one year in advance of the experiments, to allow the soil to settle from any installation disturbance. Tensiometers were installed at three soil depths, 20, 50 and 80 cm, in the upper, middle and lower part of the experimental plot. Nine tensiometers were fitted with pressure transducers, which were coded as follows: U20, U50, U80; M20, M50, M80; and L20, L50, and L80 for the upper, middle and lower part of the experimental block at 20, 50 and 80 cm of soil depth, respectively. Tensiometers without pressure transducers were installed to insure the existence of at least one operational unit at each location. Calibration and performance of the pressure transducers and mercury-water manometers are reported elsewhere (Návar, 1992).

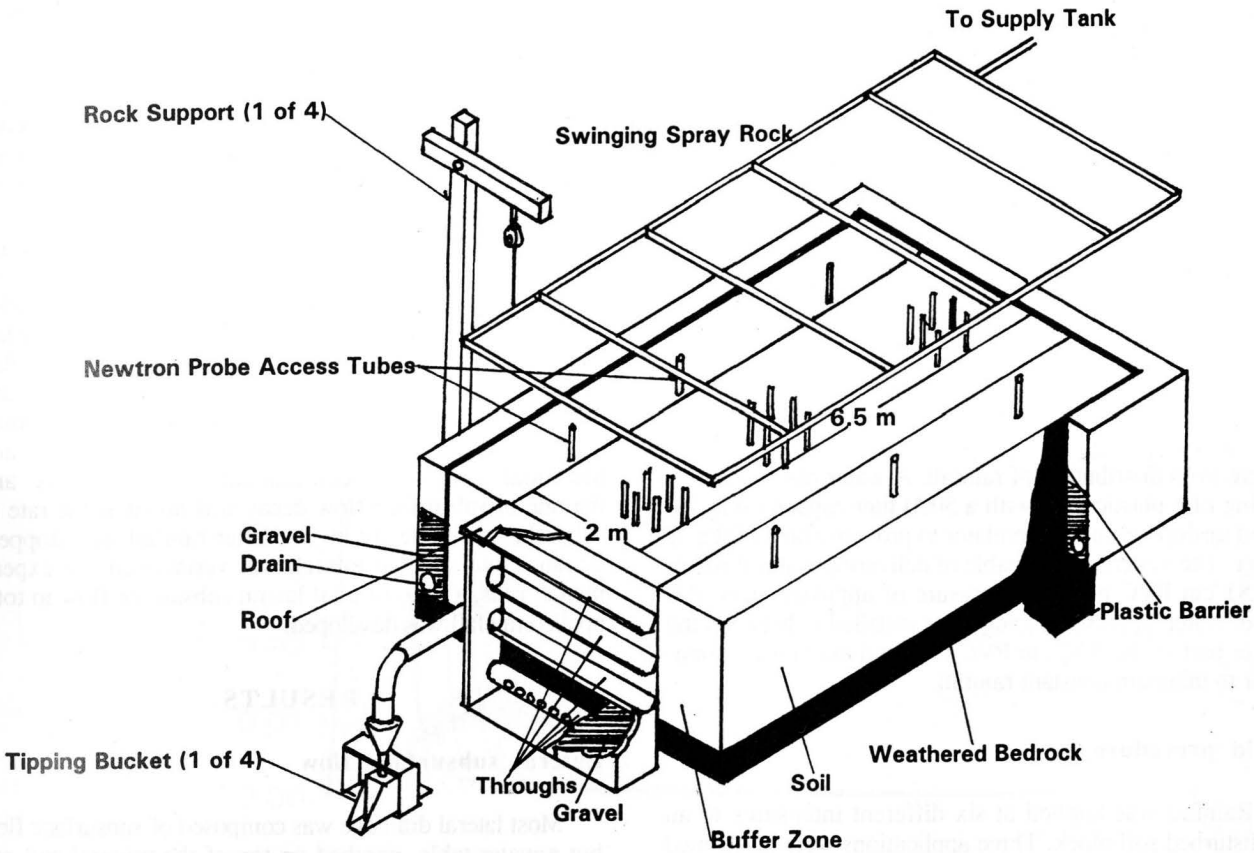

Fig. 1. Schematic drawing of the experimental layout and the soil block.

Table 1

Some soil characteristics of the experimental plot.

Soil profile	Soil depth (cm)	Soil description	Soil sand (%)	texture Clay (%)	Silt (%)	Soil bult density ($grcm^{-3}$)
01	2.5-3.5	Forest litter				
02	0.0-2.5	Mull layer of partially decomposed organic matter				
A1	0.0-2.5	Pale brown (10YR 6/3) loam				
E	2.5-10	Light yellowish (10YR 6/4) loam				
Bt1	10-22	Yellowish brown (10YR 5/6)	19.7	34.4	45.9	1.31
Bt21	23-43	Yellowish brown (10YR 5/8)	32.7	24.7	42.8	1.47
Bt22	43-63	Yellowish brown (10YR 5/8) clay				
B3	63-81	Mottled red clay	39.7	17.8	42.5	1.60
C	81-102	Moderately weathered shale rock and clay soil material				

The description of soil profiles was carried out by USDA Forest Service (1964). The textural and soil bulk density analyses were conducted by the author.

Soil moisture contents

Soil moisture content was measured with sentry 200 probes. Probes were placed at 20, 50 and 80 cm of soil depth in the middle and upper part of the experimental plot. Factory calibration for each probe was used to estimate soil moisture content on volume per volume basis.

Bromide observations

Bromide is a tracer, nontoxic to animals commonly found in the Ouachita National Forest, non-sorbed nor chemically or biologically altered and easy to quantify (Levy and Chambers, 1987). Samples of lateral subsurface flow taken during the first applied rain storm indicated that

Br^- was not present naturally. Bromide concentrations in subsurface flow were measured with a Br^- ion selective electrode with a double junction reference electrode. Probe calibration was continuously recorded by measuring a standard solution having a Br^- concentration in the range of the sample concentrations.

Rainfall simulator

The rainfall simulator consisted of a rectangular frame made of 1.905 cm diameter PVC pipe with spraying nozzles placed underneath. The industrial spraying nozzles (Lechler from Jackson and Associates) produced a full cone axial spray pattern. The number and type of nozzles varied according to a specific rainfall intensity. The rainfall simulator was suspended by ropes and swung back and forth to insure even distribution of rainfall. A water reservoir consisting of a plastic tank with a 5000 liter capacity was located upslope from the simulator to provide gravity feed of water. The system was capable of delivering water through a 3.81 cm PVC pipe at a pressure of approximately 700 cm of water. A pressure gauge was installed in between the lower part of the 3.81 cm PVC pipe and the rainfall simulator to maintain constant rainfall.

Field procedure

Rainfall was applied at six different intensities to an undisturbed soil block. Three applications were performed at each rainfall intensity. Bromide tracer was added to the first application at a given intensity. The following two applications contained no Br^- (Additional details on the bromide experiments are reported in Turton *et al.*, 1995). A total of 7 applied storms were observed for bromide concentrations in subsurface flow. Rainfall applications ranged in depth and duration from 8.26 to 4.04 cm and 0.82 to 4.25 hours, respectively (Table 2). The rate of rainfall input varied from 7.5 to 1.04 cm h^{-1}. Applied rainfalls continued until changes in the rates of lateral subsurface flow and soil pressures became negligible. Soil water pressures from pressure transducers and subsurface flow discharge from each collector were automatically recorded with a Data Logger 21x at one minute intervals during applied rainfalls and for a 2-hour period thereafter. Thereafter, data were recorded at 10 minute intervals. Water samples, to be analyzed for bromide concentrations, were taken by hand from the subsurface flow collectors before entering the tipping bucket system every 3- to 5-min intervals. Mercury-water manometer and soil moisture content readings were taken every two to four minutes during rainfall application. Total rainfall input was measured with a set of 10 rain cans set up on the experimental plot.

Data analysis

Several regression equations, relating hydrograph parameters, the rate of applied rainfall and pre-storm soil water pressure, which met the probability requirements: $P>F \leq 0.01$, were developed. The randomized analysis of variance was also used for some hydrograph parameters and soil water pressures. The probabilities are briefly reported in the results section. Before using the statistical analysis, hydrograph parameters or soil water pressure were tested for normality using the Shapiro Wilks statistic. Mean values were denoted as follows: x=mean, x_g=geometric mean, x_m=median, and sd=root mean square or standard deviation. The subsurface hydrograph parameters used in this report were estimated as follows: the time to start subsurface flow was recorded as the lag time between the initiation of applied rainfall and initiation of subsurface flow, time of concentration or time to peak subsurface flow was recorded as the lag time between the initiation of applied rainfall and the steady subsurface flow rate, peakflow was recorded as the maximum rate of subsurface flow per minute at each soil horizon, the time to decay subsurface flow was noted as the lag time between the end of rainfall simulation and the initial decay of the constant subsurface flow rate, and the rate of subsurface flow decay was noted as the rate of subsurface flow decay in time after rainfall was stopped. Because total applied rainfall was variable among experimental runs, a ratio of total lateral subsurface flow to total applied rainfall was developed.

RESULTS

Lateral subsurface flow

Most lateral drainage was composed of subsurface flow but a water table, perched on top of the mineral soil and below the litter layer, was observed at the end of the application of the most intense rainfalls (1, 2, and 3) downslope of the experimental plot. Total produced subsurface flow hydrographs for all 17 applied storms were highly variable (Figure 2). Several hydrograph parameters such as total volume, peakflow rates, time to start and time to peak were statistically related to the rate of applied rainfall and to pre-storm soil water potential. Total lateral subsurface flow decayed at a high rate soon after rainfall was stopped.

The ratio of total lateral subsurface flow to total rainfall input and the rate of applied rainfall and pre-storm soil water potential best fitted a power relationship ($\ln Y = .9415 + .6419\ (\ln R.I.) - .434\ (\ln S.W.P)$ $r^2=0.88$, s.d=0.127 $P>F=0.00001$; Figure 5). The rate of total lateral subsurface flow increases rapidly with small increments in the rate of applied rainfall. Further increments in rainfall intensity result in lower increments in the rate of subsurface flow. The capacity of the pore system to discharge soil water becomes limiting with high rates of applied rainfall. Pre-storm soil water pressures also controlled the ratio of total lateral subsurface flow in a similar manner to that described above. However, the ratio of total lateral subsurface flow was more sensitive to changes in pre-storm soil water pressures because this range of observed values was from -10 to -100 cm of water, whereas the range of applied rainfalls varied from 1.04 to 7.3 cm h^{-1}. Plots of the ratio described before versus the rate of applied rainfall for the other soil horizons did not show statistically significant trends.

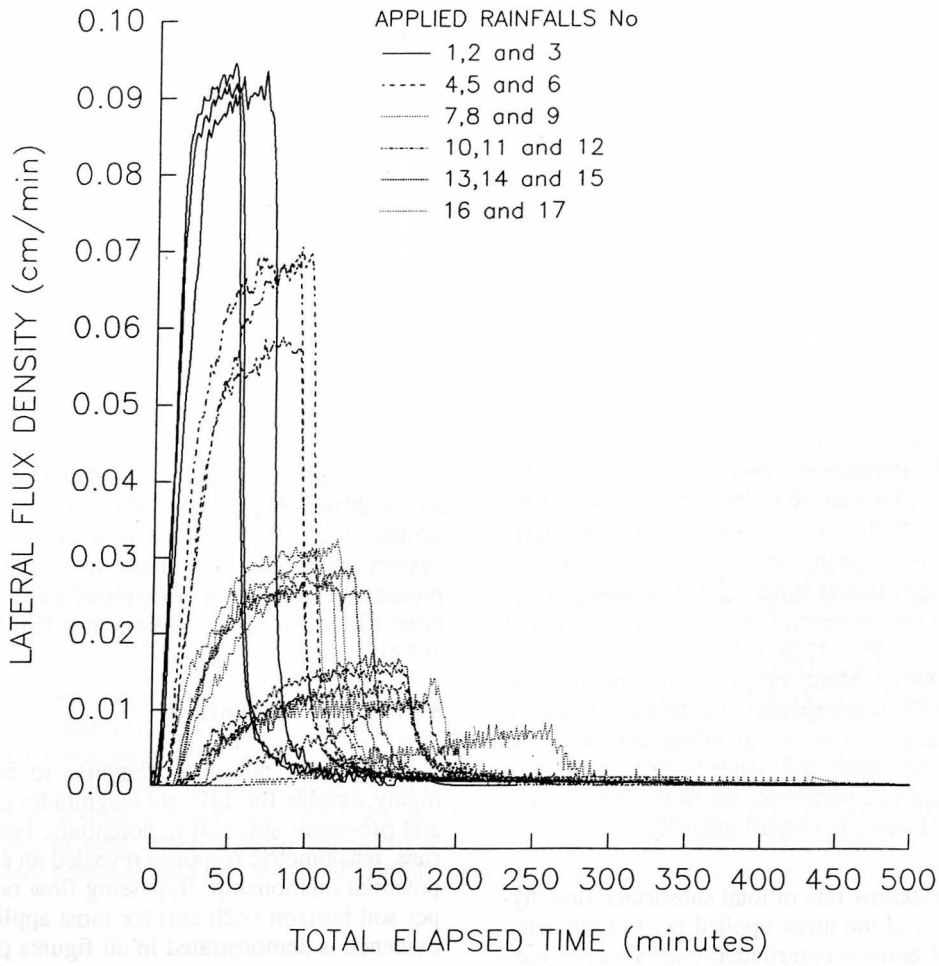

Fig. 2. Total lateral subsurface flow hydrographs for 17 applied rainfalls of different duration and intensity.

Table 2

Some characteristics of applied rainfalls.

RUN	DATE	RAIN AMOUNT (cm)	C.V. (%)	SIMULATION TIME (hrs)	RAIN INTENSITY (cm/h)	RETURN PERIOD (years)
1	07/17/91	8.26	68	1.22	6.80	20.00
2	07/24/91	5.64		0.90	6.27	4.00
3	07/25/91	6.12	22	0.82	7.49	5.00
4	07/31/91	8.41	22	1.55	5.43	10.00
5	08/01/91	7.63	25	1.67	4.58	6.00
6	08/02/91	6.70	14	1.55	4.32	5.00
7	08/06/91	6.47	27	2.00	3.23	3.00
8	08/07/91	5.79	18	1.75	3.31	3.00
9	08/08/91	5.37	14	1.92	2.80	1.50
10	08/28/91	4.78	17	3.00	1.59	1.00
11	08/29/91	4.46	10	2.75	1.62	1.00
12	08/30/91	4.65	15	2.75	1.69	1.00
13	09/10/91	5.08	29	2.75	1.85	1.00
14	09/11/91	6.26	16	2.33	2.68	2.00
15	09/12/91	5.77	17	2.17	2.66	1.80
16	10/08/91	4.42	12	4.25	1.04	1.00
17	10/09/91	4.04	21	3.08	1.31	1.00

The A&Litter soil horizon discharged a mean of 36.7 and 67.6 %, B1 4.5 and 8.9 %, B2 2.2 and 4.9 %, and B3 8.4 and 18.9 % of the total rainfall input and of the total lateral discharge, respectively. Total lateral subsurface flow from the upper soil horizon was, however, the most variable among storms. The coefficient of variation for the ratio of total subsurface flow per soil horizon to total rainfall input decreased with soil depth: from 42.5% in the A& Litter to 14.3% in the B3 soil horizon. These observations are consistent with the findings of Williams (1990) and Turton *et al.* (1992) who observed that the upper soil horizon was the most responsive and the most variable to natural rainfall events in forest soils of the Ouachita Mountains.

The A&Litter soil horizon responded soonest to applied rainfall ($P>F\leq0.05$). Because the lower B3 soil horizon responded faster (x_g=23.9 min) than the upper B2 soil horizon (x_g=28.9 min) ($P>F\leq0.05$), bypassing flow through preferential soil places was an active subsurface flow process. The time to start lateral subsurface flow was statistically related to the rate of rainfall input and pre-storm soil water potential (11.2446-0.372R.I-0.75 S.W.P, sd= 3.36, r^2=0.94, $P>F\leq0.0001$). Most variation in time to start subsurface flow, 76%, was explained by the rate of rainfall input. However, time to start lateral subsurface flow was more sensitive to pre-storm soil water potentials because changes in the latter soil parameter are more important in the equation than changes in rainfall intensity.

The average peakflow rate of total subsurface flow hydrographs was 63% of the mean applied rainfall intensity. The A&Litter soil horizon contributed with a mean peakflow rate of 75.44%, B1 with 9.40%, B2 with 3.86% and B3 with 11.29% of the total lateral subsurface flow rate. Peakflows for each soil horizon showed a great deal of variation among storms, which was partially explained by the rate of applied rainfall. Peakflows and the rate of applied rainfall fitted better polynomial, logarithmic, logarithmic and linear relationships for the A&Litter, B1, B2, and B3 soil horizons, respectively. The statistical relationships show that the capacity of the active soil pore system in drainage proceses is highly dynamic among storms and becomes limiting with high rates of rainfall application.

Time to peak was also variable among storms (x_g=64.73 min, sd=54.45 min). The rate of applied rainfall and pre-storm soil water potential partially explained the variation of time to peak (46.13-0.354 R.I-0.7804 S.W.P, sd=9.46, r^2=0.97, $P>F\leq0.0001$). Intense applied rainfalls on low pre-storm soil water potentials resulted in the smallest time to peak. Time to start was, however, more sensitive to soil water potential than to the rate of rainfall input. That is, time to peak changes are more noticeable with changes in soil water potential than with changes in the rate of rainfall application. Time to peak lateral subsurface flow was linearly related to time to peak (34.4+1.04* (time to start), sd=0.02, r^2=0.99 $P>F\leq 0.0001$). The slope, 1.04, is dimensionless (time time^{-1}), whereas the intercept has a time dimension, (minutes) and may physically explain the time factor to fully activate the soil pore system contributing to subsurface flow processes.

The time to decay subsurface flow physically explains the time needed to deactivate part of the most active pore system, macropores with very little interaction with the soil matrix with a direct inlet-outlet. This parameter resulted in the following pattern: x_m=2.0, x_g=3.6, x_g=7.5 and x_g=6.5 min for the A&Litter, B1, B2 and B3, respectively. The rate of subsurface flow hydrograph decay was also very sensitive to the rate of rainfall application. Total subsurface flow hydrographs receded to approximately 80 % of their peakflow rate in approximately 15 minutes after stopping rainfall. The quick response of subsurface flow hydrographs to stopping rainfall and the fast rate of hydrograph decay indicated that the active soil pore system comprises a small portion of the total soil pore system, consistent with the observations of Luxmoore *et al.*, (1990) and Jardine *et al.*, (1990). That is, a small portion of the soil system appears to participate in lateral subsurface flow processes. This process of subsurface flow generation has been called the 'faucet-like water flow' (Mosley, 1979, 1982).

Soil water potentials

Soil water potential response to rainfall input was highly variable for different magnitudes of applied rainfalls and pre-storm soil matric potentials. For all experimental runs, tensiometric response revealed an erratic infiltration-potential relationship. Bypassing flow occurred in the upper soil horizon (<20 cm) for most applied rainfalls. This evidence is demonstrated in all figures plotting the development of soil water potentials during the application of rainfall (Figures 3a, tU80, 3b4, tM50 and tM80, 3c, tL50 and tL80 4b, tM50 and tM80, and 4c, tL50 and tL80; tensiometers below 20 cm of soil depth responded instantaneously to rainfall application with no lags with soil depth). In general, tensiometers placed at 50 or 80 and 80 cm of soil depth consistently responded faster 20% and 35% of the time than tensiometers placed at 20 and 50cm of soil depth, respectively. Therefore, lateral unsaturated flow was common in the experimental plot. Unsaturated lateral flow occurred in 13 out of 17 experimental runs in the upper soil horizon and it started during all 17 storms despite 70% of tensiometers showing negative soil water potentials.

Perched water tables developed quickly at all soil depths for all applied storms; note the positive soil water potentials for all tensiometric data. Transition from negative to positive soil water potential occurred most of the time before 50 minutes of rainfall application. Rainfall intensity controlled the time of transition, intense applied rainfalls (1,2,3,4,5, and 6) resulted in quick and less intense applied rainfalls (9,10,11,16, and 17) resulted in slow transitions from negative to positive soil water potentials. In the middle and upper part of the experimental plot, perched water tables developed first at 50 cm for the least intense applied rainfalls. In the lower part of the experimental plot, perched water tables developed first at 20 cm of soil depth

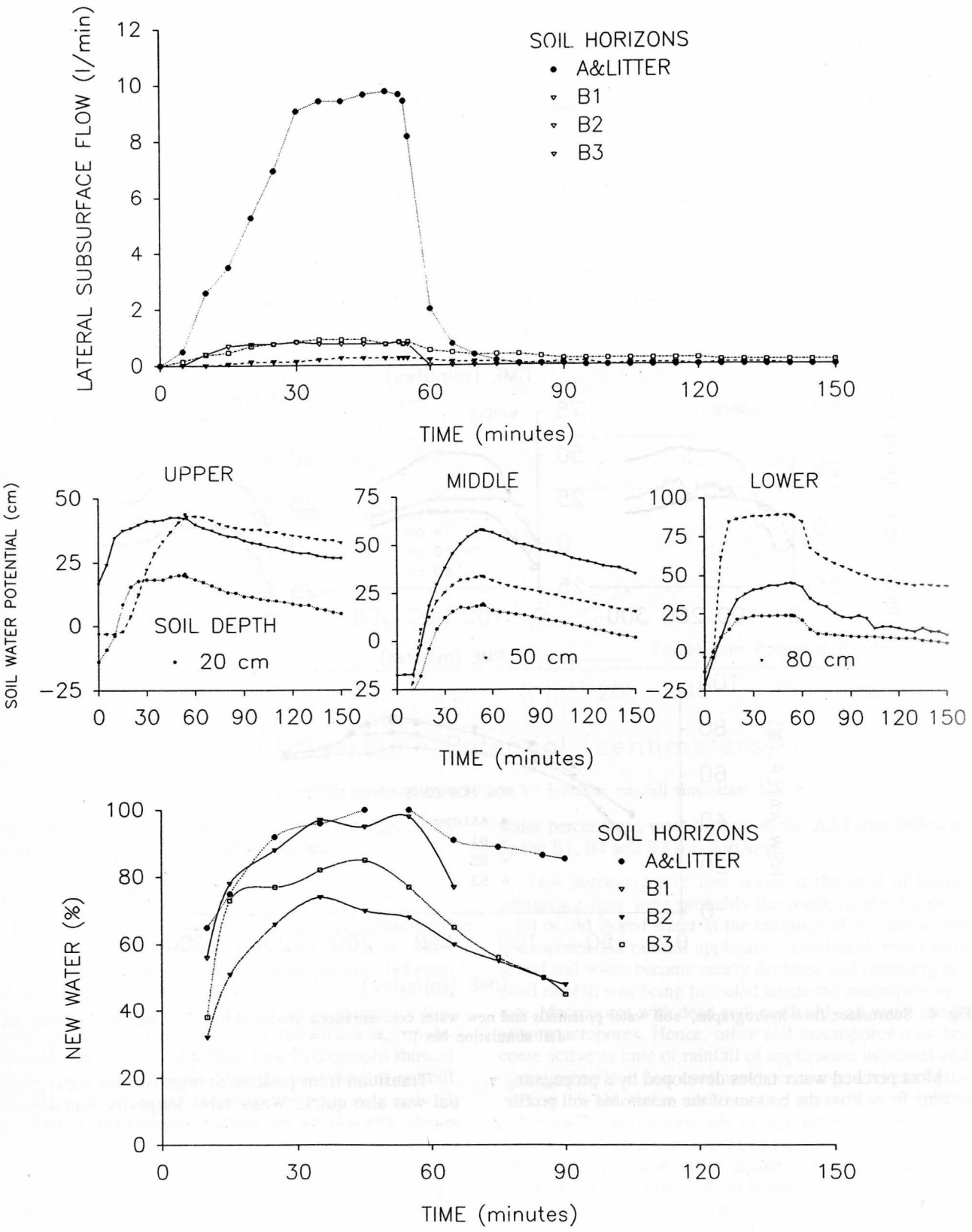

Fig. 3. Subsurface flow hydrographs, soil water potental and new water concentrations produced by a 63 mm h^{-1} intensity rainfall simulation No 2.

for applied rainfalls with intensities less than 2 cm h^{-1}. For applied rainfalls with intensities larger than 3 cm h^{-1}, there is no conclusive evidence about which soil depth first developed a perched water table.

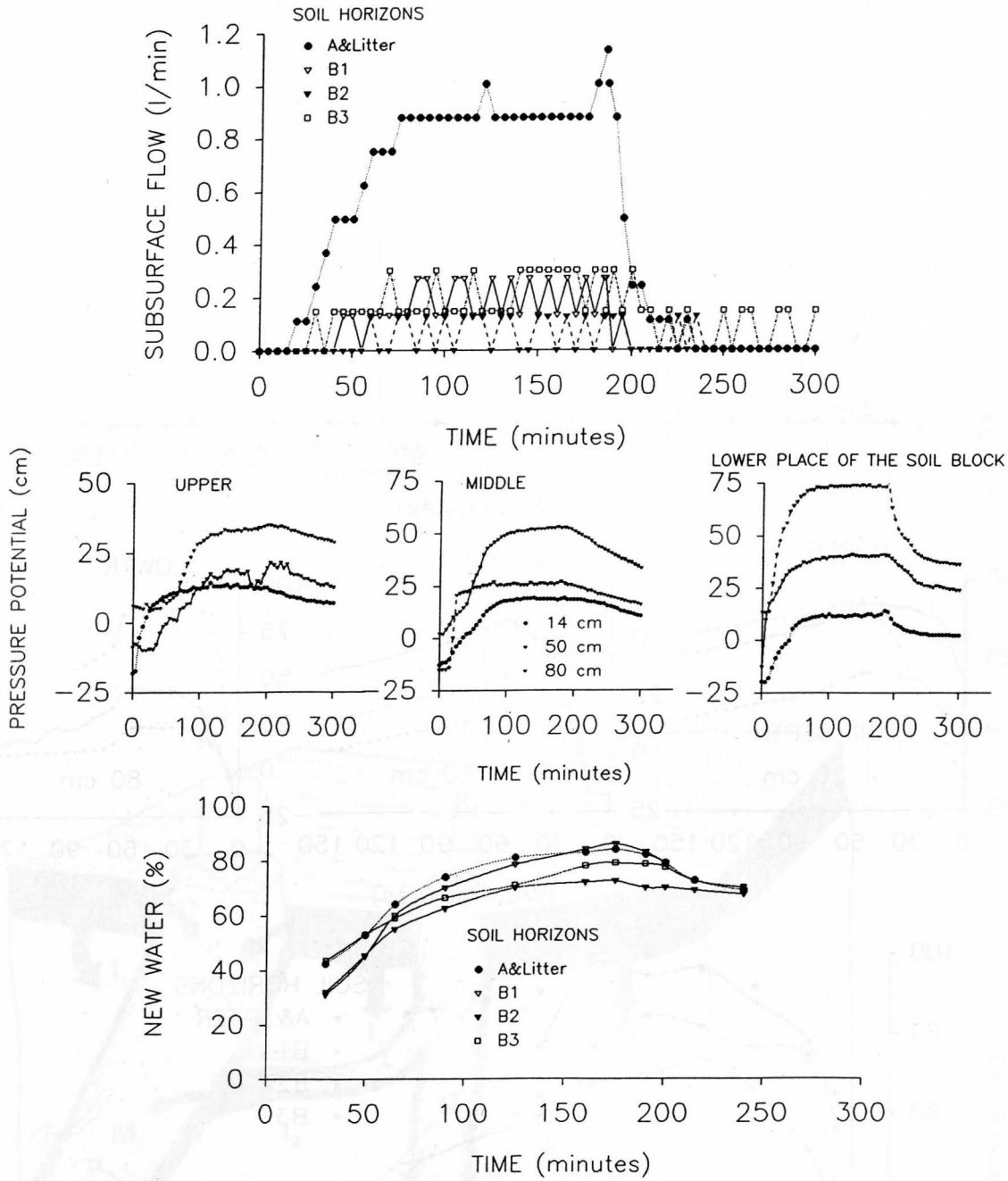

Fig. 4. Subsurface flow hydrographs, soil water potentials and new water concentrations produced by a 13.1 mm h^{-1} intensity rainfall simulation No 17.

Most perched water tables developed by a propagating wetting front from the bottom of the monitored soil profile rather than from the top of the soil profile (Figure 5). Consequently the soil profile between tensiometers exhibited an unrequited soil matrix. At the time of ceasing rainfall, the soil water potential profiles appeared to attain an infiltration-potential relationship, the slope of the potential soil profile was similar to the slope of the equilibrium potential gradient, for intense applied rainfalls for the lower and middle part of the experimental plot. For less intense applied rainfalls, the middle and lower part of the experimental plot exhibited an erratic infiltration-potential relationship.

Transition from positive to negative soil water potential was also quick. Water table longevity was approximately 300 min for the shallow mineral soil (<50 cm of soil depth) and 1400 min for the bottom soil profile. Perched water tables mimicked subsurface flow hydrographs (Figure 3) indicating that drainage was very efficient. By the time subsurface flow hydrographs had receded at 14, 23 and 45 cm of soil depth, low magnitude-perched water tables remained at 20 and 50 cm of soil depth and they supplied subsurface flow to the bottom 80 cm of the soil profile. The low magnitude-perched water tables showed again unrequited soil zones in between. For example, three unrequited soil zones were observed 60 minutes

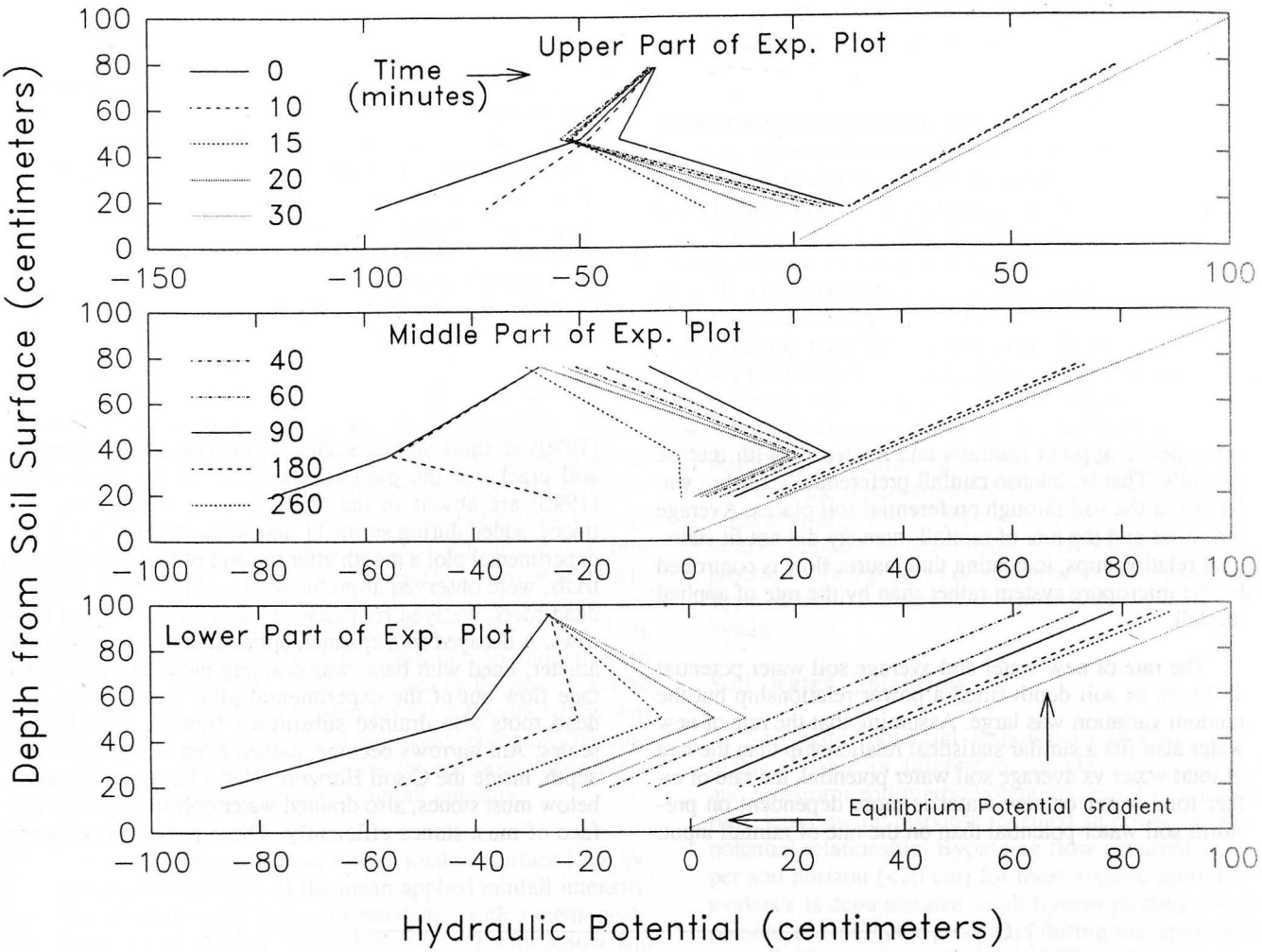

Fig. 5. Soil water potentials produced by a 10 mm h^{-1} intensity rainfall simulation No 16.

after stopping rainfall: 1) the top 12 cm, 2) between 20-35 cm, and 3) between 45-50 cm of soil depth.

New water vs old water

Lateral subsurface flow showed large concentrations of new water for all applied storms (Figures 3c and 4c). New water concentrations displayed similar patterns between soil depths and between applied rainfalls and mimicked most lateral subsurface flow hydrographs, except for low pre-storm soil water potential. For the former soil moisture conditions, lateral subsurface flow hydrographs showed high new water percentages from the beginning of rainfall application. New water percentages were lowest early in subsurface flow processes (approximately 62% for the sum of all soil depths), except for low pre-storm soil water potentials and intense applied rainfalls. The percentage of new water attained an average of approximately 85% of the total lateral subsurface flow. The time to peak new water concentrations was the same as the time to peak total lateral subsurface flow. However, at the end of a particular applied storm, maximum new water percentages attained 100% in the uppermost responsive soil depth and 72% for the lowest soil horizon (44 cm), respectively. Although the variations between soil horizons were minimal, new water percentages were highest in the A&Litter followed by the B1, B4 and B3 soil horizons.

Low percentages of new water at the start of lateral subsurface flow were probably the result of the displacement of old stored water at the entrance of the active soil macropores. As rainfall application continued, previously stored soil water became nearly depleted and incoming applied rainfall was being funneled inside the macropore system. Macropores with dead ends push old soil water inside other macropores. Hence, other soil macropores may become active as time of rainfall of application increases and lateral subsurface flow continues increasing, whereas a proportion of old water continues to contribute to lateral subsurface flow. Therefore, the final subsurface flow rate and its chemistry are dependent on the number and size of active macropores as well as on the hydraulic conductivity of the soil matrix between macropores. Old water concentrations at the end of the rainfall applications may come from water displaced in the soil matrix by potential flow processes and the depletion of new water inside the macropore system. That is, new water concentrations decay after stopping rainfall, indicating that rainfall input is directly contributing to most subsurface flow through preferential soil macropores. New water in the macropore system be-

comes rapidly depleted and old, stored water continues to contribute to lateral subsurface flow at a slow, nearly constant rate.

Average new water for all soil horizons and the rate of applied rainfall fitted a logarithmic relationship well (Figure 6). That is, preferential flow as well as total lateral subsurface flow are controlled by the rate of rainfall input as indicated before and observed also by Ehlers (1975) and Edwards *et al.*, (1992) in macropores of soils of agricultural lands. Total new water was approximately 76 % of the total rainfall input and attained approximately 85 % of the total lateral subsurface flow. The latter percentage diminishes with a reduction in the rate of rainfall application and increases with an increment in the rate of applied rainfall, indicating that the rate of old soil water increases with less intense applied rainfalls and decreases with intense rainfalls. That is, intense rainfall preferentially flushes water out of the soil through preferential soil places. Average old water and the rate of rainfall intensity did not fit statistical relationships, indicating that matrix flow is controlled by the micropore system rather than by the rate of applied rainfall.

The rate of new water and average soil water potential at 20 cm of soil depth fitted a power relationship but the random variation was large. Assuming that the rate of new water also fits a similar statistical relationship than the rate of total water vs average soil water potential, the rate of either total water or new water is more dependent on prestorm soil water potential than on the rate of rainfall input.

DISCUSSION

Evidence has been presented that macropore, channeling, short circuiting or bypassing flow (Bouma, 1990; Beven and Germann, 1982; Wilson and Luxmoore, 1988 and Watson and Luxmoore, 1986) is an active subsurface flow process in the experimental forest plot. New water percentages dominated subsurface flow hydrographs, erratic infiltration-potential relationships were observed in most tensiometers, unsaturated subsurface flow was a common drainage process and unrequited soil zones developed between perched water tables in the experimental plot.

Macropore flow processes observed in this experimental forest plot are similar to those outlined by McDonnell (1990) at short spatial scales. However, soil fissures or soil cracks of the dimensions observed by McDonnell (1990) are absent in the studied soils. Rhodamine dye traces, added during storm 11 and while digging the entire experimental plot a month after the end of the experimental trials, were observed at preferential soil places: living and dead roots, decayed root channels and worm and ant burrows. A decayed root channel, approximately 2.5 cm in diameter, lined with bark, was draining most lateral subsurface flow out of the experimental plot. Small living and dead roots also drained subsurface flow at short spatial scales. Ant burrows become stained even at 90 cm of soil depth, inside the C soil Horizon. Worm burrows, observed below most stones, also drained water collected on the surface of most stones efficiently. These passageways were

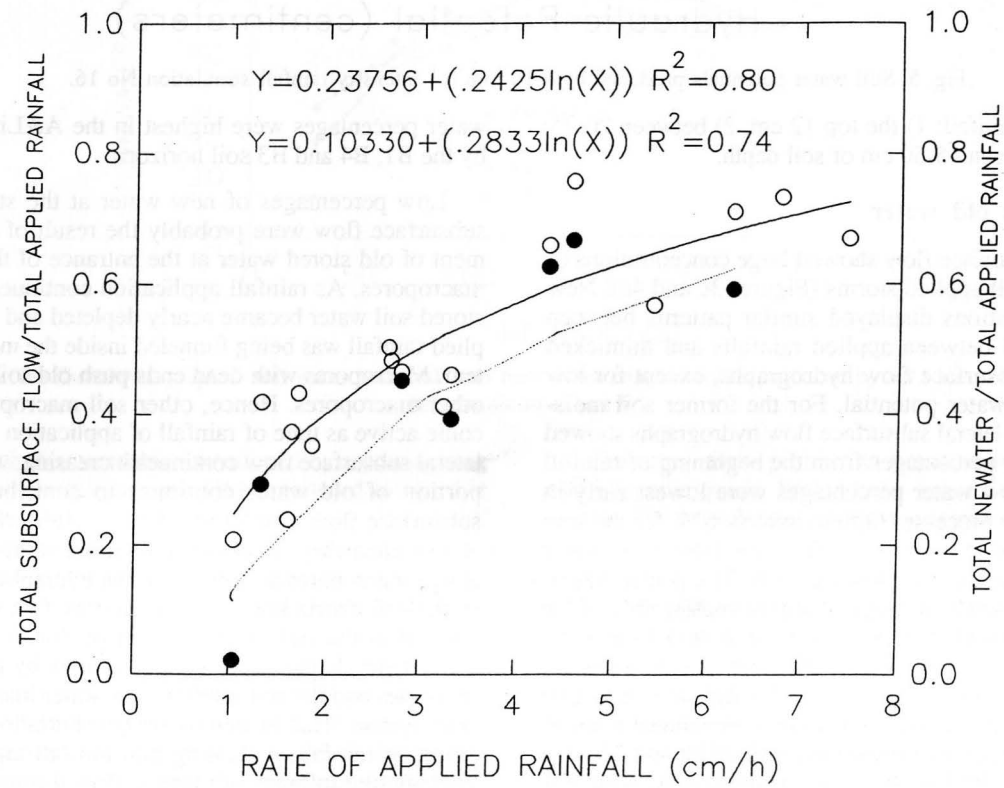

Fig. 6. The dependence of the ratio of total subsurface flow and total new water to total rainfall input on the rate of applied rainfall.

also observed to contribute to bypass flow at short spatial scales. However, most stained water passageways were observed above the interface of the A & B soil horizons. This finding is also consistent with the total lateral subsurface flow observed above the interface of these soil horizons. That is, drainage occurs as shallow subsurface flow, consistent with the observations of Turton *et al.*, (1992), Williams, (1990) and McDonnell *et al.*, (1991).

This wealth of information can be graphically represented in the spatial model of Figure 7. The model indicates that macropore flow is driven by rainfall intensity and soil water potential. The interactions of these parameters became obvious during the application of storms No 16 and 17, the least intense applied rainfalls. Less intense applied rainfalls on low soil water potentials can produce lateral subsurface flow with limited interactions with the huge amount of stored water in the soil. Rainfall No 17, which was applied at a rate of 3.6×10^{-3} cm sec^{-1} on an average soil water potential of -17 cm of water and average soil moisture deficit of 0.25 cm cm^{-1} at the uppermost responsive soil horizon, generated approximately 68% of new water as lateral subsurface flow. On the other hand, storm No 16, which was applied at a rate of 2.88×10^{-4} cm sec^{-1} on average soil water potentials of -100 cm of water and 0.21 cm cm^{-1} of soil moisture content in the upper most responsive soil horizon, generated approximately 13% of new water as lateral subsurface flow.

Intense applied storms on similar soil water potentials also provide soil water to flow preferentially inside the macropore system. Storms No 2, 6, and 9, which were applied at a rate of 1.75×10^{-3}, 1.86×10^{-3}, and 1.49×10^{-3} cm sec^{-1}, respectively, on average soil water potentials of -20 cm of water and soil moisture content of 0.25 cm cm^{-1}, generated approximately 65%, 94 and 91% of new water, respectively.

Considering that none of the storms were applied with intensities smaller than the saturated hydraulic conductivity

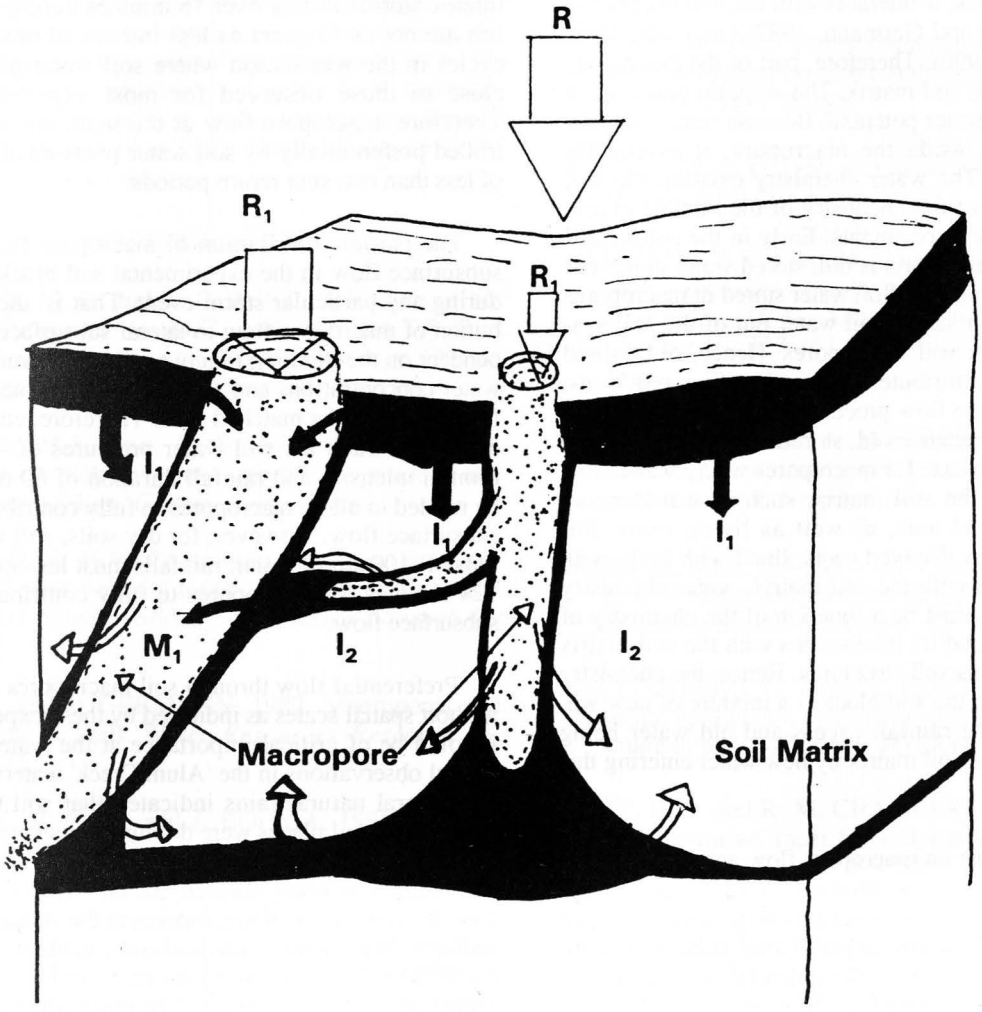

Fig. 7. Conceptual model of macropore flow generation at short spatial scales in the experimental soil block. (R=Rainfall, R_1=Rainfall input into macropores: rainfall collected on matted leaves, stones, branches located on top of the soil; I_1=Infiltration into the soil matrix ($f(\psi,k(\psi))$; I_2=Infiltration into the macropore system ($f(\psi=0)$ and $R/k_{sat}(\psi=0)>0$); I_3= Infiltration from macropores to the soil matrix ($f(\psi,k(\psi))$; M_1= Macropore flow). Where: ψ=soil water potential, $k(\psi)$=Unsaturated hydraulic conductivity, k_{sat}=saturated hydraulic conductivity. Note: 1) the unrequited soil zones between soil macropores and 2) the activation process of other soil macropores.

for the matrix system, estimated by Návar *et al.*, (1995) on the same experimental soil block as 6.6 x 10^{-4} cm sec^{-1}, some of the rainfall input entered the mesopore system (Watson and Luxmoore, 1986 and Wilson and Luxmoore, 1988) and the macropore system (Germann and Beven, 1982). Therefore, the ratio between the rate of rainfall input over the saturated hydraulic conductivity, of the soil matrix, is the rainfall excess. The rainfall excess must partially explain the rate of new water entering the macropore system of soils and the high new water concentrations and high rates of lateral subsurface flow observed in these experiments.

Rainfall excess must flow preferentially in the macropore system, which advances ahead of the potential wetting front (Figure 7) because macropore flow velocity is of a magnitude several times larger than matrix flow (Kluitenberg and Horton, 1989 and Andreini and Steenhuis, 1990) and the author (Návar *et al.*, 1995) estimated an average macropore flow velocity of 4.2 x 10^{-2} cm sec^{-1}, approximately 70 times larger than matrix flow. As water flows inside the macropores, it interacts with the soil matrix (as observed by Beven and Germann, 1982; Germann, 1986 and Jardine *et al.*, 1990). Therefore, part of the macropore flow is sorbed by the soil matrix. The sorption process is a function of the soil water potential. Because rainfall excess continues to flow inside the macropore, it eventually reaches the outlet. The water chemistry existing the soil block is a function of the chemistry of the rainfall excess as observed in these experiments. Early in the subsurface flow process, rainfall excess is old, stored water at the entrance of most macropores. Soil water stored in macropores with dead ends push stored soil water out of the soil system activating other soil macropores. Hence, old, stored water continues to contribute to subsurface flow processes. Late in the subsurface flow process, rainfall excess is new, incoming rainfall, because old, stored water is eventually depleted. This is the case for macropores where water flow is in contact with the soil matrix, such as soil burrows made by worms and ants, as well as living roots. For macropores made by decayed roots, lined with bark, with limited interactions with the soil matrix, water chemistry reaching the outlet must be a function of the chemistry of the rainfall excess and its interactions with the soil matrix at the entrance of this soil structures. Hence, the chemistry of the water leaving the soil block is a mixture of new water coming from the rainfall excess and old water being flushed out from the soil matrix by new water entering this soil system.

The observations on macropore flow and water chemistry by the bromide concentrations must be considered cautiously because the soil water potentials and the rate of applied storms during the experimental runs were conducive to the observation of the potential contribution of macropores to lateral subsurface flow, as well as the interactions between macropore and matrix flow. Several applied rainfalls had larger than 1 year return periods and the soil block had less than -100 cm of soil water potential or approximately 0.21 cm cm^{-1}, because evapotranspiration was curtailed by eliminating plant cover. That is, although most of the environmental conditions outlined above are not so frequent for the observation of the full contribution of macropore flow at the spatial scale studied for this report, several of them are present on annual basis in forest soils of the Ouachita Mountains of Arkansas.

Soil water potentials observed during the experimental runs are more frequently encountered in The Ouachita Mountains than the rate and duration of most applied storms. Low soil water potentials are common during wet cycles in the low evapotranspiration season (March, April and May, when most streamflow is generated, Miller *et al.*, 1988, Williams, 1990). Therefore, storms with less than 1 year return periods, storms No 16 and 17, would generate macropore flow at the experimental plot scale if they last longer than 25 minutes. During the dry season, July and August, macropore flow could contribute to lateral subsurface flow in the experimental plot when intense rainfalls, such as applied storms No 1, 2, and 3, generate enough rainfall excess. These storms must last longer than 75 minutes to observe macropore flow at short spatial scales. Intense storms lasting over 75 minutes during the dry season are not as frequent as less intense storms during wet cycles in the wet season where soil water potentials are close to those observed for most experimental runs. Therefore, macropore flow at the scale observed is controlled preferentially by soil water pressure at time scales of less than one year return periods.

The partial contribution of macropore flow to lateral subsurface flow in the experimental soil block is dynamic during any particular storm event. That is, the full contribution of macropore flow to lateral subsurface flow is dependent on the duration of any particular storm event. New water concentrations and time to peak the total subsurface flow hydrographs matched well. Therefore, environmental conditions such as: soil water pressures of -20 cm, any rainfall intensity and rainfall duration of 60 minus would be needed to allow macropores to fully contribute to lateral subsurface flow. However, for dry soils, soil water potentials of -100 cm of water, rainfalls must last approximately 124 minutes for macropores to fully contribute to lateral subsurface flow.

Preferential flow through soil macropores is important at short spatial scales as indicated by these experiments and it could be of critical importance at the watershed scale. Visual observations in the 'Alum Creek' watershed 11 during several natural rains indicated that soil fissures and preferential soil places were draining considerable amounts of soil water. The water temperature indicated that stored, soil water was being flushed out the mineral soil. Therefore, the continuity of macropores at the watershed scale is unlikely. Macropores with dead ends, as observed inside the experimental plot, must push old, stored, water out, activating other soil macropores. Therefore water and chemical transport through macropores may be spatially limited at the watershed scale. Hence, soil water translation mechanisms as those observed by McDonnell (1990) may be also controlling subsurface flow at the watershed scale in forested soils of the Ouachita Mountains. These subsurface

flow processes are critical to understand the temporal variations in streamflow chemistry.

CONCLUSIONS

The dependence of most lateral subsurface flow hydrograph parameters on rainfall intensity and pre-storm soil water potential, the unsaturated subsurface flow, the irregular wetting and drying fronts and the high percentages of new water in subsurface flow indicated that drainage in the experimental soil block is highly transient. Therefore other approaches, combined with potential flow, must be considered when physically modelling subsurface flow in forested watersheds in the Ouachita Mountains of Arkansas at short spatial scales.

ACKNOWLEDGMENTS

This report is part of a Ph.D. dissertation at Oklahoma State University. The work was supported by the US Forest Service Southern Forest Experiment Station, Oxford, MS (Coop Agreement 19-88-065), the Weyerhaeuser Company Southern Forest Research Center, Hot Springs, AR and the Oklahoma Agricultural Experiment Station. We thank all those who were involved in this work and especially Michael Kress and Gary Miller for their assistance in the field and lab, as well as M.Sc. Patricia Grounds for the revision of the manuscript.

BIBLIOGRAPHY

ANDERSON, M. G. and T. P. BURT, 1990. Subsurface Runoff Processes. *In*: M.G. Anderson and T.P. Burt (Eds). Process Studies in Hillslope Hydrology. Chapter 11, 365-400. John Wiley & Sons Ltd. New York.

ANDREINI, M.S. and T. S. STEENHUIS, 1990. Preferential paths of flow under conventional and conservation tillage. *Geoderma 46*, 85-102.

BEASLEY, R. S. 1976. Contribution of subsurface flow from the upper slopes of forested watersheds to channel flow. *Soil Science Society of America Journal 40*, 955-957.

BEVEN, K. and P. GERMANN, 1982. Macropores and water flow in soils. *Water Resources Research 18*, 1311-1325.

BOOLTINK, H. W. G. and J. BOUMA, 1991. Physical and morphological characterization of bypass flow in a well-structured clay soil. *Soil Science Society of American Journal, 55*, 1249-1254.

BOUMA, J. 1990. Using morphometric expressions for macropores to improve soil physical analyses of field soils. *Geoderma, 46*, 3-11.

CASSEL, D. K. and A. KLUTE, 1986. Water potential: tensiometry. *In*: A. Klute (Ed) Methods of Soil Analysis, Part I. 2nd ed. Agronomy, 563-596.

DEWITT, J. N. and E. C. STEINBRENNER, 1981. Central Arkansas Soil Survey. Weyerhaeuser Co. Tacoma, WA.

DUNNE, T. and R. D. BLACK, 1970a. An experimental investigation of runoff production in permeable soils. *Water Resources Research, 6*, 478-490.

DUNNE, T. and R. D. BLACK, 1970b. Partial area contributions to storm runoff in a small New England watershed. *Water Resources Research, 6*, 1296-1311.

DUNNE, T. and L.B. LEOPOLD, 1978. Water in Environmental Planning. W. H. Freeman and Company. San Francisco, CA.

EDWARDS, W.M., M. J. SHIPITALO, W.A. DICK and L.B. OWENS, 1992. Rainfall intensity affects transport of water and chemicals through macropores in no-till soil. *Soil Science Society of America Journal, 56*, 52-58.

EHLERS, W. 1975. Observations on earthworm channels and infiltration on tilled and untilled loess soil. *Soil Science, 119*, 242-249.

GERMANN, P. F. 1986. Rapid response to precipitation. *Hydrological Processes, 1*, 3-13.

GERMANN, P. F. 1990. Macropores and hydrologic hillslope processes. *In*: Process Studies in Hillslope Hydrology. M. G. Anderson and T. P. Burt. (Eds). Chapter 10, 327-363. John Wiley & Sons Ltd. New York.

HEWLETT, J. D. and A. R. HIBBERT, 1963. Moisture and energy conditions within a sloping soil mass during drainage. *J. Geophys. Res., 68*, 1081-1087.

JARDINE, P.M., G.V. WILSON and R.J. LUXMOORE, 1990. Unsaturated transport through a forest soil during rain storm events. *Geoderma, 46*, 103-118.

KLUITENBERG, G. J. and R. HORTON, 1990. Effect of solute application method on preferential transport of solute in soil. *Geoderma, 46*, 283-297.

LEVY, B. S. and R. M. CHAMBERS, 1987. Bromide as a conservative tracer for soil-water studies. *Hydrologiacal Proceedings, 1*, 385-389.

LUXMOORE, R. J., P. M. JARDINE, G. V. WILSON, J. R. JONES and L. W. ZELANY, 1990. Physical and chemical controls of preferred path flow through a forested hillslope. *Geoderma, 46*, 139-154.

McDONNELL, J. J., 1990. A rationale for old water discharge through macropores in a steep humid catchment. *Water Resources Research, 26*, 2821-2832.

McDONNELL, J. J., I. F. OWEN and M. K. STEWART, 1991. A case study of shallow flow paths in a steep zero-order basin. *Water Resources Bulletin, 27*, 4, 679-685.

MILLER, E. L., R. S. BEASLEY and E. R. LAWSON, 1988. Forest Harvest and site preparation effects on stormflow and peakflow of ephemeral streams in the Ouachita Mountains. *Journal of Environmental Quality 17*, 212-218.

MOSLEY, M. P. 1979. Streamflow generation in forested watersheds, New Zealand. *Water Resources Research, 15*, 795-806.

MOSLEY, M. P., 1982. Subsurface flow velocities through selected forest soils, south island, New Zealand. *J. Hydrol., 55*, 65-92.

NAVAR, J., 1992. Water movement in an experimental in the Ouachita Mountains of Arkansas: the effect of soil macropores. Ph.D. Dissertation. Oklahoma State University.

NAVAR, J., D. J. TURTON and E. MILLER, 1995. Estimating the relative importance of macropore and matrix flow by using the hydrograph separation procedure in an experimental plot in the Ouachita Mountains of Arkansas. *Hydrological processes, 9*, 743-753.

SKLASH, M. G., M. K. STEWART and A. J. PEARCE, 1986. Storm runoff generation in humid headwater catchments: II. A case study of hillslope and low-order stream response. *Water Resources Research, 22*, 1273-1282.

TURTON, D. J., T. C. HAAN and E. L. MILLER, 1992. Subsurface flow responses of a small forested catchment in the Ouachita Mountains. *Hydrological Processes, 6*, 111-125.

U. S. D. A. FOREST SERVICE, 1964. Special soil survey report of Alum Creek Experimental Forest Ouachita National Forest, Sabine County, AR.

WHIPKEY, R. Z., 1965. Subsurface stormflow from forested watersheds. *Bulletin International Association Scientific Hydrology, 10*, 74-85.

WATSON, K. W. and R. J. LUXMOORE, 1986. Estimating macroporosity in a forest watershed by use of a tension infiltrometer. *Soil Science Society American Journal, 50*, 578-582.

WILLIAMS, M. A., 1990. Saturated interflow and water table response of a small forested watershed in the Ouachita Mountains of Central Arkansas. M.Sc. Thesis. Oklahoma State University.

WILSON, G.V. and R.J. LUXMOORE, 1988. Infiltration and macroporosity distributions on two forested watersheds. *Soil Science Society American Journal, 52*, 329-335.

José Návar[1], Edwin L. Miller[2] and Donald J. Turton[2]

[1] *Facultad de Ciencias Forestales, Universidad Autónoma de Nuevo León, Apartado Postal # 136, 67700 Linares, N.L.*

[2] *Dept of Forestry, Oklahoma State Univ., Stillwater, OK 74078.*